Adaptive Rejection of Disturbances Having Two Sinusoidal Components with Close and Unknown Frequencies

Xiuyan Guo and Marc Bodson

Abstract—The paper considers the problem of rejecting disturbances composed of two sinusoidal signals with frequencies that are close to each other. A natural approach consists in treating the two components separately. However, when the frequencies are close and unknown, the convergence of a double frequency estimator is typically slow, due to the difficulty in distinguishing the components. The alternative approach taken in this paper consists in representing the disturbance signal as a single sinusoid with time-varying magnitude and phase. The theoretical basis and the limitations of such a representation are first discussed. Then, an adaptive disturbance rejection algorithm is proposed and the resulting nonlinear system is analyzed using various approximations. Simulation results show that the proposed algorithm has better convergence properties than an algorithm designed to cancel the two frequency components separately. In some cases, however, the cost is a small residual error.

I. INTRODUCTION

The rejection of periodic disturbances is a common problem in control and signal processing applications. While the known frequency case is well understood, techniques to handle unknown and time-varying frequencies have only recently emerged. Indirect methods perform disturbance rejection by estimating the frequency of the disturbance and using the estimate in an algorithm designed for a known frequency [2]. In contrast, direct methods attempt to design a stable adaptive controller for the rejection of the disturbance [1] [2]. Note that the problem of extracting a periodic signal from noisy data can be cast in a disturbance rejection framework by letting the plant be a unity operator. In other words, signal reconstruction can be viewed as a special case of disturbance rejection.

Recently, researchers have considered problems where the frequencies of two independent sinusoidal signals must be tracked, including cases where the two frequencies are very close. For example, [4] describes a problem where a sensor must be developed to measure mass flow in an agricultural machine. The spectrum of the sensor data shows a peak at 13.2 Hz, corresponding to the mass flow, together with a parasitic signal at 11.6 Hz, corresponding to the resonance frequency of the sensor. In [6], the problem of pitch tracking for automatic music transcription is considered. When multiple notes are played together (polyphonic case), the algorithm must track more than one sinusoidal

component. The paper reports data for notes at 262 Hz and 392 Hz, but closer spacing may be encountered. In [5], the disturbance rejection problem is considered for a web transport application. The frequencies of the disturbances originating from the winding and unwinding rolls merge and split as functions of time.

Disturbance rejection can be performed by using an adaptive scheme with parallel structure. In [3], a signal reconstruction method was proposed to track two closely-spaced sinusoids. Two identical estimators were combined to account for the two components. Precautions were taken to prevent the two frequency estimates from converging to the same values. However, a problem for algorithms with parallel structure is that the convergence may be very slow when the frequencies are close.

It is known from communications theory that a sinusoid that is amplitude-modulated by a sinusoid of lower frequency has a spectrum reflecting the presence of two sinusoids with close frequencies. The same is true, approximately and under similar conditions, for frequency-modulated signals. This paper is based on the reverse property that a pair of sinusoids can be represented as a single sinusoid with time-varying magnitude and phase. The observation is used to develop an adaptive disturbance rejection scheme, and its advantages over a double/parallel algorithm are investigated in simulations.

II. REPRESENTING TWO SINUSOIDS AS A SINGLE TIME-VARYING SINUSOID

Consider a signal with two sinusoidal components

$$d(k) = m_1 \cos(\omega_1 k + \phi_1) + m_2 \cos(\omega_2 k + \phi_2) \quad (1)$$

where m_1, m_2 are the magnitudes of the two components, ω_1, ω_2 are their frequencies, and ϕ_1, ϕ_2 are their initial phases. Let

$$
\begin{aligned}
\alpha_f(k) &= \frac{(\omega_1 + \omega_2)k + \phi_1 + \phi_2}{2} \\
\alpha_s(k) &= \frac{(\omega_1 - \omega_2)k + \phi_1 - \phi_2}{2}
\end{aligned}
\quad (2)
$$

and define the associated frequencies

$$\omega_f = \frac{\omega_1 + \omega_2}{2}, \; \omega_s = \frac{\omega_1 - \omega_2}{2} \quad (3)$$

Note that, if ω_1 and ω_2 are close to each other, ω_s is much smaller than ω_f. Accordingly, we will call ω_f the *fast frequency* and ω_s the *slow frequency*.

To lighten the notation in the following presentation, we will drop the time index k from α_f and α_s. However, the reader should remember that they remain functions of time. The following fact forms the basis of the paper.

Fact: the signal in (1) can be represented as a time-varying sinusoid in the form

$$
\begin{aligned}
d(k) &= m_d(k)\cos(\alpha_d(k)) \\
\alpha_d(k) &= \alpha_f(k) + \phi(k)
\end{aligned}
\tag{4}
$$

where

$$
m_d(k) = \sqrt{m_1^2 + m_2^2 + 2m_1 m_2 \cos(2\alpha_s)}
\tag{5}
$$

$$
\phi(k) = \arctan\left((m_1 - m_2)\sin\alpha_s, (m_1 + m_2)\cos\alpha_s\right)
\tag{6}
$$

The parameters m_d and ϕ of (5), (6) will be called the *nominal parameters*.

An alternative expression is

$$
m_d(k) = \sqrt{m_1^2 + m_2^2 + 2m_1 m_2 \cos(2\alpha_s)}\,\mathrm{sign}(\cos\alpha_s)
\tag{7}
$$

$$
\begin{aligned}
\phi(k) &= \arctan\left((m_1 - m_2)\sin\alpha_s, (m_1 + m_2)\cos\alpha_s\right) \\
&\quad - \frac{1 - \mathrm{sign}(\cos\alpha_s)}{2}\pi
\end{aligned}
\tag{8}
$$

The parameters m_d and ϕ of (7), (8) will be called the *alternative parameters*.

Proof: from the definitions of α_f, α_s, the signal in (1) can be written as

$$
d(k) = m_1\cos(\alpha_f + \alpha_s) + m_2\cos(\alpha_f - \alpha_s)
\tag{9}
$$

Therefore

$$
\begin{aligned}
d(k) &= (m_1 + m_2)\cos\alpha_s\cos\alpha_f - \\
&\quad (m_1 - m_2)\sin\alpha_s\sin\alpha_f
\end{aligned}
\tag{10}
$$

Eq. (4) is obtained if $m_d(k)$ and $\phi(k)$ are chosen such that

$$
\begin{aligned}
(m_1 + m_2)\cos\alpha_s &= m_d(k)\cos(\phi(k)) \\
(m_1 - m_2)\sin\alpha_s &= m_d(k)\sin(\phi(k))
\end{aligned}
\tag{11}
$$

Indeed, for $m_d(k)$ as defined in (5), and for $\phi(k)$ as defined in (6), (11) holds. Therefore, (5) and (6) are valid. The alternative expression with (7), (8) follows directly from this result. □

The fact indicates that a signal composed of two sinusoids can always be represented as a single sinusoid with time-varying parameters. If the frequencies of the two components are close, the magnitude m_d and the phase ϕ are periodic and vary at the frequency ω_s that is lower than the primary frequency ω_f. Fig. 1 shows an example where $m_1 = 2$ and $m_2 = 1$. The figure shows both the magnitude and the phase of the time-varying sinusoid as a function of α_s. If the frequencies are $\omega_1 = 0.01 \times 2\pi$ and $\omega_2 = 0.011 \times 2\pi$, the fast frequency is $\omega_f = 0.0105 \times 2\pi$ (corresponding to a period of about 95 samples) and the slow frequency is $\omega_s = 0.0005 \times 2\pi$ (corresponding to a
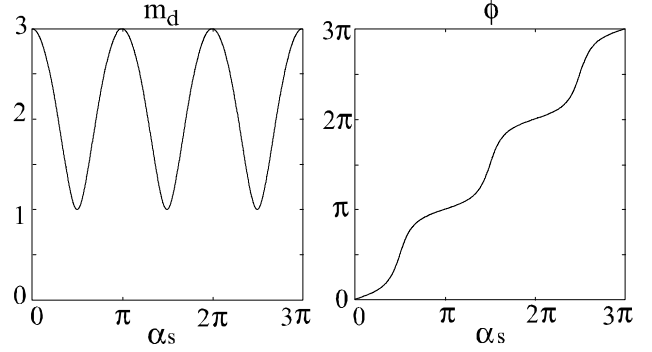
Fig. 1. Example with $m_1 = 2$ and $m_2 = 1$ and nominal parameters
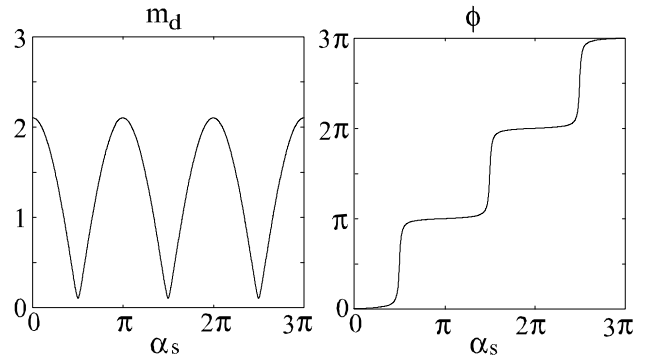
Fig. 2. Example with $m_1 = 1.1$ and $m_2 = 1$ and nominal parameters

period of 2000 samples). The oscillations in the magnitude and phase of the time-varying sinusoid are about 21 times slower than the primary frequency.

Unfortunately, while the magnitude and the phase parameters are periodic at the slow frequency, they may exhibit rapid changes. At such times, a system designed to track the parameters (such as a phase-locked loop) will have difficulties maintaining a small error. Rapid changes occur especially when $m_1 \simeq m_2$. Fig. 2 shows an example where $m_1 = 1.1$ and $m_2 = 1$ and the parameters of the time-varying sinusoid are specified by (5) and (6). The phase ϕ shows abrupt changes near $\alpha_s = \pi/2$, $3\pi/2$, and $5\pi/2$. In the extreme case where $m_1 = m_2$, the magnitude parameter becomes the absolute value of a sinusoid of frequency ω_s and the phase is a staircase signal that jumps by π when the magnitude is zero. It is constant otherwise.

The limiting case where $m_1 = m_2$ is the motivation for the alternative parameters of (7) and (8). This formulation lets the magnitude parameter change sign, so that the phase parameter is equal to zero for all time. Both parameters are much smoother functions of time. When m_1 and m_2 are close but not equal, the alternative parameters are not as smooth, but nevertheless smoother than the nominal parameters. Fig. 3 shows the alternative parameters when $m_1 = 1.1$ and $m_2 = 1$. Note that m_d is discontinuous when $\alpha_s = \pi/2$, $3\pi/2$, and $5\pi/2$, but the jumps are small because
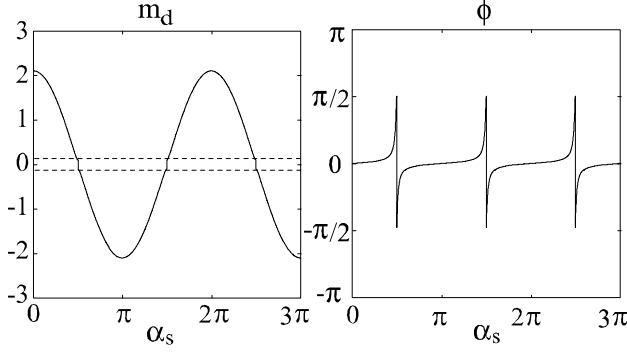
Fig. 3. Example with $m_1 = 1.1$ and $m_2 = 1$ and alternative parameters

$m_1 \simeq m_2$ (between $|m_1 - m_2| = 0.1$ and $-|m_1 - m_2| = -0.1$) and the slope of the signal is smoother. The phase parameter exhibits rapid changes, but instead of a large jump, one finds a glitch of short duration. Further, the glitch occurs when the signal has small magnitude. Therefore, a system with limited bandwidth, such as a phase-locked loop, will "ride through" the glitch, with only a small impact on performance.

III. ADAPTIVE ALGORITHM

A. Adaptive algorithm

We propose a new disturbance rejection algorithm based on the scheme of [1]. The disturbance rejection scheme is shown as an add-on to a nominal controller with transfer function $C(z)$. In particular, we show how the algorithm can track a pair of sinusoidal disturbances as a single, time-varying sinusoid, and how the algorithm can be modified to improve performance when $m_1 \simeq m_2$. The structure of the proposed disturbance rejection system is shown in Fig. 4.

The plant is described by

$$y(z) = P(z)(u_c(z) + u_d(z) - d(z)) \tag{12}$$
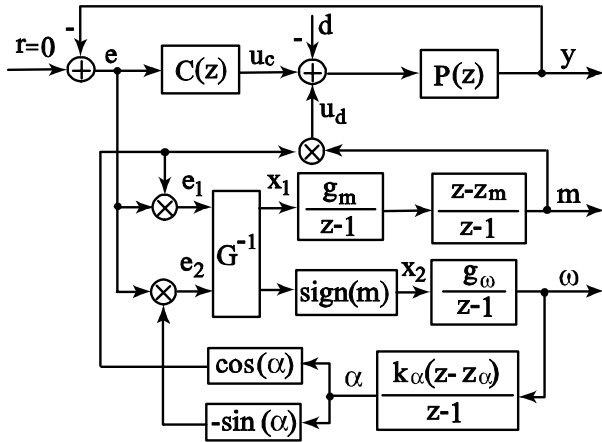
Fig. 4. Adaptive algorithm for the rejection of a sinusoidal disturbance with time-varying magnitude and phase

where $P(z)$ is the plant transfer function, $u_c(z)$, $u_d(z)$ and $d(z)$ are the z-transforms of the controller output, of the disturbance compensation signal, and of the input disturbance, respectively. The disturbance d has the form of (1) with instantaneous frequency

$$\omega_d(k) = \omega_f + \phi(k) - \phi(k-1) \tag{13}$$

where ω_f is defined in (3) and ϕ in (6) or (8).

The disturbance compensation signal has the form

$$u_d(k) = m(k)\cos(\alpha(k)) \tag{14}$$

where the magnitude m is the estimate of m_d and the phase α is the estimate of the phase α_d. The signal ω is an estimate of ω_d. The equations of the algorithm in Fig. 4 are

$$\begin{array}{rcl} \begin{bmatrix} x_1 \\ x_2 \end{bmatrix} & = & \begin{bmatrix} 1 & 0 \\ 0 & \text{sign}(m) \end{bmatrix} G^{-1} \begin{bmatrix} e\cos(\alpha) \\ -e\sin(\alpha) \end{bmatrix} \\ u_d(k) & = & m(k)\cos(\alpha(k)) \end{array} \tag{15}$$

where G is a 2×2 matrix

$$G = \frac{1}{2} \begin{bmatrix} G_R & -G_I \\ G_I & G_R \end{bmatrix} \tag{16}$$

and G_R and G_I are the real and imaginary parts of the following frequency responses, evaluated at the nominal frequency ω_d

$$\begin{array}{rcl} G_R & = & \text{Re}[\dfrac{P(e^{j\omega_d})}{1 + P(e^{j\omega_d})C(e^{j\omega_d})}] \\ G_I & = & \text{Im}[\dfrac{P(e^{j\omega_d})}{1 + P(e^{j\omega_d})C(e^{j\omega_d})}] \end{array} \tag{17}$$

The remaining signals are given in the z-domain by

$$\begin{array}{rcl} m(z) & = & \dfrac{g_m(z - z_m)}{(z-1)^2} x_1(z) \\ \omega(z) & = & \dfrac{g_\omega}{z-1} x_2(z) \\ \alpha(z) & = & \dfrac{k_\alpha(z - z_\alpha)}{z-1} \omega(z) \end{array} \tag{18}$$

The parameter k_α is chosen so that, for constant frequency ω, the phase α is the integral of the frequency. Thus,

$$k_\alpha = \frac{1}{1 - z_\alpha} \tag{19}$$

A significant difference between this algorithm and the algorithm of [1] is the presence of the $\text{sign}(m)$ term, which was inserted in the algorithm to allow the magnitude estimate to change sign.

B. Linear approximate analysis

We propose an analysis of the system based on a series of approximations inspired from the theory of phase-locked loops. The analysis assumes that m, m_d, ω and ω_d vary slowly. The adaptive parameters m and ω can be made to vary slowly by choosing small controller gains. The signal parameters m_d and ω_d vary slowly for large relative difference between m_1 and m_2, and for $m_1 = m_2$. For

m_1 and m_2 close but not equal, the approximation is valid, except around the discontinuity points. However, the jumps in m_d are relatively small and the short duration glitches in ϕ occur when the signal has small magnitude, so that the approximation is still useful.

Given sufficiently slow variation of the signal and adaptive parameters, the next step is to assume that the response of the plant to d and u_d can be approximated by the sinusoidal steady-state. Thus, the outputs can be computed based on the frequency response of the closed-loop system. Then, as is commonly in the theory of phase-locked loops, only the low-frequency components resulting from multiplication of two sinusoidal signals are kept in the equations. Finally, it is assumed that the instantaneous frequencies ω and ω_d are close enough that $P(e^{j\omega})$ and $C(e^{j\omega})$ can be replaced by $P(e^{j\omega_d})$ and $C(e^{j\omega_d})$.

Under above assumptions, the error signal is

$$e(k) \simeq \frac{P(e^{j\omega_d})}{1 + P(e^{j\omega_d})C(e^{j\omega_d})}\left[d - u_d\right] \quad (20)$$

Substituting (4) and (14) into (20), we can obtain

$$\begin{aligned} e(k) &\simeq& G_R m(k)\cos(\alpha_d(k)) - G_I m_d(k)\sin(\alpha_d(k)) - \\ && G_R m(k)\cos(\alpha(k)) + G_I m(k)\sin(\alpha(k)) \quad (21) \end{aligned}$$

After discarding of the high-frequency terms $\sin(2\alpha(k))$, $\cos(2\alpha(k))$, $\sin(\alpha(k)+\alpha_d(k))$, and $\cos(\alpha(k)+\alpha_d(k))$, we have

$$\begin{aligned} e_1(k) &\simeq& \frac{1}{2}G_R m_d(k)\cos(\alpha(k)-\alpha_d(k)) - \frac{1}{2}G_R m(k) \\ && +\frac{1}{2}G_I m_d(k)\sin(\alpha(k)-\alpha_d(k)) \end{aligned}$$

$$\begin{aligned} e_2(k) &\simeq& -\frac{1}{2}G_R m_d(k)\sin(\alpha(k)-\alpha_d(k)) - \frac{1}{2}G_I m(k) \\ && +\frac{1}{2}G_I m_d(k)\cos(\alpha(k)-\alpha_d(k)) \quad (22) \end{aligned}$$

The discarding is justified both by m_d and m varying sufficiently slowly and by the low-pass filtering. A vector form of (22) is given by

$$\begin{bmatrix} e_1 \\ e_2 \end{bmatrix} \simeq G \begin{bmatrix} m_d(k)\cos(\alpha(k)-\alpha_d(k)) - m(k) \\ -m_d(k)\sin(\alpha(k)-\alpha_d(k)) \end{bmatrix} \quad (23)$$

For small phase error, $\cos(\alpha(k)-\alpha_d(k)) \simeq 1$, $\sin(\alpha(k)-\alpha_d(k)) \simeq \alpha(k) - \alpha_d(k)$, and we obtain

$$\begin{bmatrix} x_1 \\ x_2 \end{bmatrix} \simeq \begin{bmatrix} m_d(k) - m(k) \\ \text{sign}(m)m_d(k)(\alpha_d(k) - \alpha(k)) \end{bmatrix} \quad (24)$$

If the magnitude estimate tracks the magnitude signal well, $\text{sign}(m) \times m_d(k) \simeq |m_d(k)|$ leads to

$$\begin{bmatrix} x_1 \\ x_2 \end{bmatrix} \simeq \begin{bmatrix} m_d(k) - m(k) \\ |m_d(k)|(\alpha_d(k) - \alpha(k)) \end{bmatrix} \quad (25)$$

Therefore, the dynamics of the system become decoupled, and the decoupled linear approximations of the frequency loop and of the magnitude loop are shown in Fig. 5 and Fig. 6. Note that G^{-1} in Fig. 4 cancels the phase shift induced by the closed-loop transfer function.
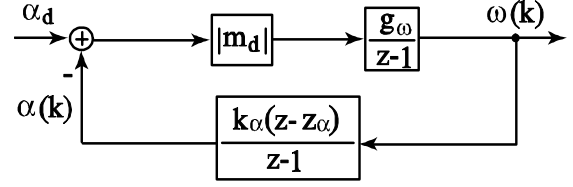
Fig. 5. Linear approximation of the frequency estimation loop
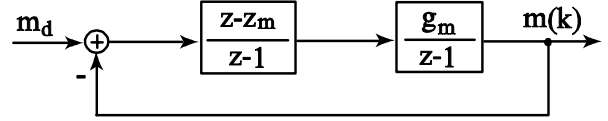
Fig. 6. Linear approximation of the magnitude estimation loop

C. Parameter design principles

For the approximate frequency loop in Fig. 5, the poles of the closed-loop system can be placed by appropriate choice of the controller parameters. For $z_{d,\omega}$ some desired location in the z plane (inside the unit circle), the following parameters will result in poles at that location

$$\begin{aligned} g_\omega &=& \frac{(1 - z_{d,\omega})^2}{|m_d|} \\ z_\alpha &=& \frac{1 + z_{d,\omega}}{2} \quad (26) \end{aligned}$$

For the magnitude loop in Fig. 6, if $z_{d,m}$ is the desired location of the poles, it is possible to place the two closed-loop poles at $z_{d,m}$ by letting

$$\begin{aligned} g_m &=& 1 - z_{d,m} \\ z_m &=& \frac{1 + z_{d,m}}{2} \quad (27) \end{aligned}$$

To implement the algorithm, initial estimates of the magnitude and the frequency of the disturbance should be used. They should be used to set the initial parameters g_ω and G^{-1}, which may then be updated as functions of m and ω, or be kept unchanged during the adaptation if the prior estimates are sufficiently precise.

It should be noted that this algorithm cannot achieve zero output error, even in the ideal case (where no measurement noise or plant uncertainty is added to the system). However, the error will be small if the parameter variation is slow. The worst case occurs when m_1 and m_2 are close to each other but not equal. Simulations show that, even in this worst case, the algorithm can suppress most of the disturbance. If more performance is needed, a parallel structure should be used. However, although the parallel structure can achieve zero output error in the ideal case, the convergence rate is slower, as will be seen from the simulation results in Section IV.

IV. SIMULATION RESULTS

To demonstrate the fast convergence rate of the algorithm, we first consider a signal reconstruction problem and
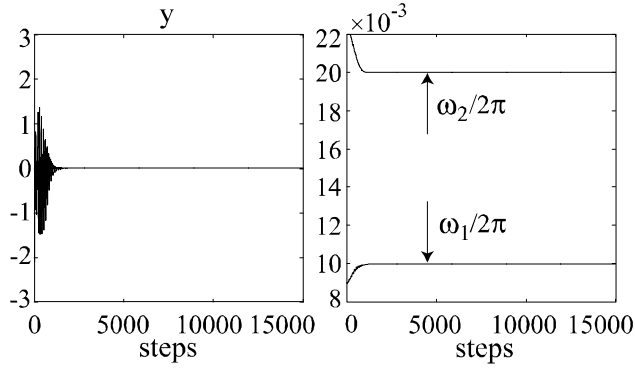
Fig. 7. The error signal and two frequency estimates: widely separated frequencies and large adaptation gain case
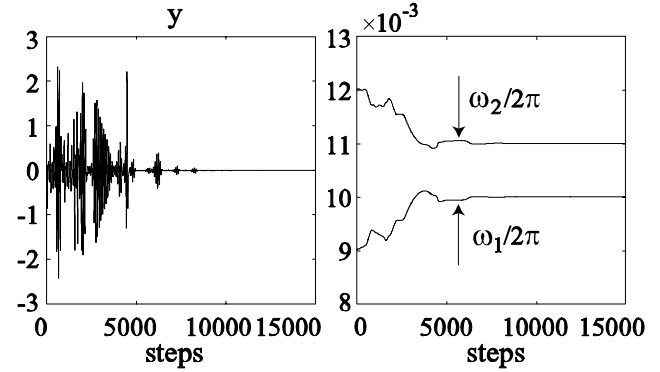
Fig. 9. The error signal and two frequency estimates: closely spaced frequencies and small adaptation gain case
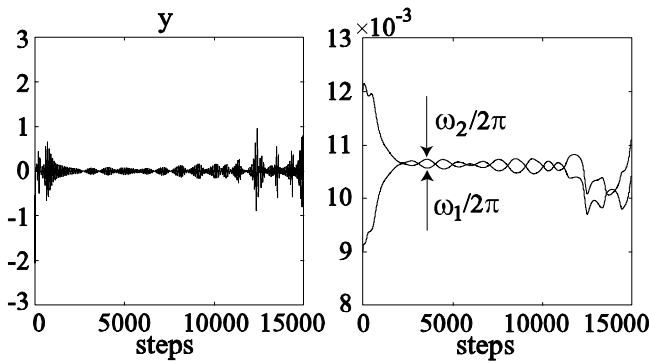
Fig. 8. The error signal and two frequency estimates: closely spaced frequencies and large adaptation gain case
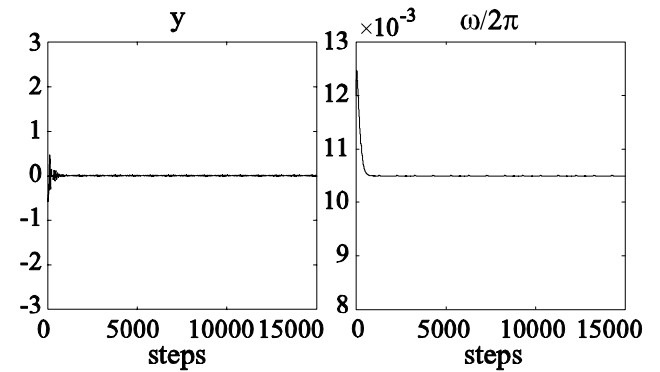
Fig. 10. The error signal and frequency estimate: our scheme for plant $p(z) = 1$ case

compare the results of the algorithm with those obtained with the double/parallel structure from [3]. The estimator for two frequencies consists of two replica of the algorithm presented in this paper, but without the sign(m) term, and with only one pole in the magnitude loop (another pole was added to improve tracking of time-varying magnitudes in this paper). Since the plant has transfer function $P(z) = 1$, the error signal $y(k) = d(k) - \hat{d}_1(k) - \hat{d}_2(k)$ is the plant output.

In the first simulation, the disturbance is $d = \cos(0.01 \times 2\pi \times k) + \cos(0.02 \times 2\pi \times k + \pi/2)$ and the initial values are $\omega_{1,0} = 0.009 \times 2\pi$, $\omega_{2,0} = 0.022 \times 2\pi$, $m_{1,0} = m_{2,0} = 1.5$, and $\alpha_{1,0} = \alpha_{2,0} = 0$. The desired closed-loop poles are $z_d = 0.995$ and $z_m = 0.95$. The separation procedure described in [3] is not used. The simulation results can be seen in Fig. 7. In contrast, Fig. 8 shows a simulation for a disturbance with much closer frequencies: $d = \cos(0.01 \times 2\pi \times k) + \cos(0.011 \times 2\pi \times k + \pi/2)$, where $\omega_{2,0} = 0.012 \times 2\pi$, and all the other parameters are the same as the simulation in Fig. 7. The two figures show that fast convergence rate is achieved for widely spaced frequencies, but difficulties occur for closely spaced frequencies. Fig. 9 shows that the problem with closely-spaced frequencies can be resolved by choosing smaller adaptation gains. The

simulation is the same as Fig. 8 except that the frequency loop poles are located at 0.998 instead of 0.995.

To demonstrate the benefit of the algorithm presented in this paper, a simulation is performed for the disturbance in Fig. 8 with $\omega_0 = 0.012 \times 2\pi$, $z_{d,\omega} = 0.99$ and the other parameters the same as the estimators in Fig. 8. In this simulation, both g_ω and G^{-1} are updated as functions of estimates m and ω. m_d of (26) is substituted by its estimate m and g_ω has an upper bound $(1 - z_{d,\omega})^2/0.01$. The results are shown in Fig. 10, where one can see that the convergence time is much less than 1000 steps, instead of about 8000 steps for the double/parallel structure (see Fig. 9). Note that the frequency estimate converges to the fast frequency $\omega_f = 0.0105 \times 2\pi$. The drawback is that there is a very small residual error in the error, associated with the time variation of the signal parameters.

We also present the results of a simulation of a disturbance rejection problem with a non-unity plant, and consider the unfavorable case where the two magnitude parameters are close but not equal. The plant is a pure delay $P(z) = z^{-10}$ and the controller $C(z) = 0$, as is typically the case for active noise control applications. The disturbance has magnitudes $m_1 = 1.1$, $m_2 = 1.0$, frequencies $\omega_1 = 0.01 \times 2\pi$, $\omega_2 = 0.011 \times 2\pi$, and initial
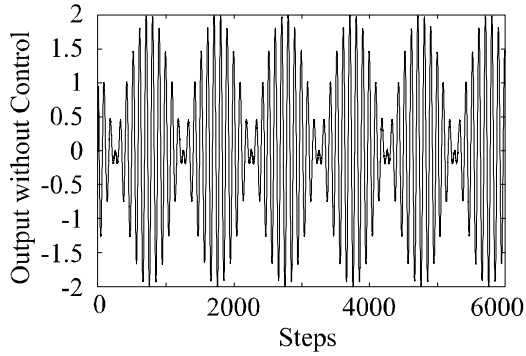
Fig. 11. Plant output without compensation
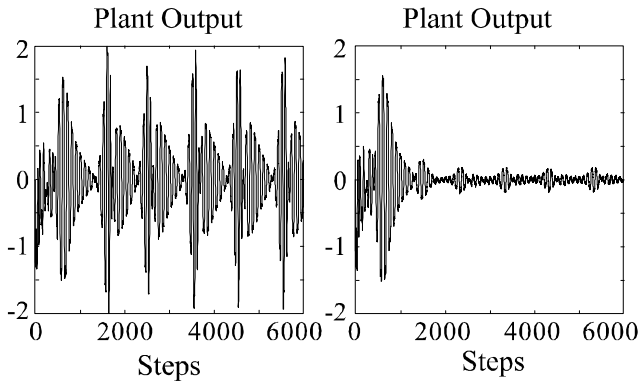
Fig. 12. Plant output: algorithm without sign(m) (left) and algorithm with sign(m) (right)

Fig. 13. Frequency estimate: without sign(m) term (left) and with sign(m) (right)
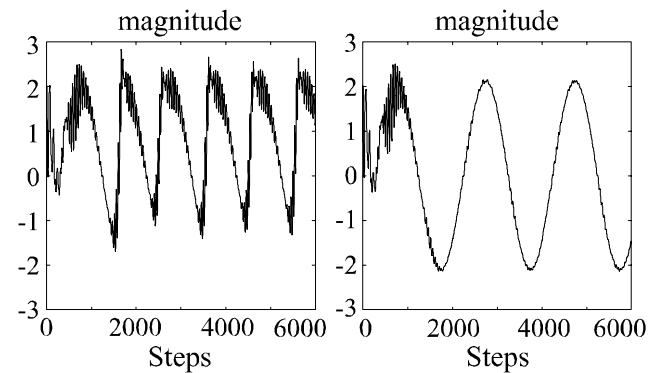
Fig. 14. Magnitude estimate: without sign(m) term (left) and with sign(m) (right)

phases $\phi_1 = 0$, $\phi_2 = \pi/2$. Moreover, additive white noise with variance $\sigma^2 = 0.01^2$ is added to the plant input. The initial value of the estimates of the algorithm are 1.5 for the magnitude, $0.012 \times 2\pi$ for the frequency and 0 for the phase. The desired closed-loop poles are selected as $z_{d,\omega} = 0.995$, $z_{d,m} = 0.95$. This leads to the parameters of the algorithm $g_m = 0.05$, $g_\omega = 1.666 \times 10^{-5}$, $z_\alpha = 0.9975$, $k_\alpha = 400$, $z_m = 0.975$. In the simulation, these parameters were kept fixed and the matrix G^{-1} was updated with the frequency estimate ω, assuming that the plant was known exactly. In order to show the effects of the sign(m) term, a simulation was also performed without the sign(m) term, leaving all the other parameters the same.

Fig. 11 gives the plant output without disturbance compensation, and Fig. 12 shows the output of the plant $y(k)$ (including the noise). The plot on the left side shows the plant output where the algorithm has no sign(m) term. A large residual disturbance is seen in the output, due to the abrupt phase changes. The right side plot, obtained with the sign(m) term, shows far smaller deviations of the plant output. Comparing Fig. 11 and Fig. 12, it is obvious that the effect of the disturbance is greatly reduced when the sign(m) term is used. A double/parallel algorithm could reduce this error further, so that choosing the algorithm of this paper is justified when fast convergence is preferred,

possibly at the cost of a small residual error. Fig. 13 and Fig. 14 give the responses of the frequency and magnitude estimates for the two cases.

REFERENCES

[1] M. Bodson, "Performance of an adaptive algorithm for sinusoidal disturbance rejection in high noise," *Automatica*, vol. 37, no. 7, 2001, pp. 1133-1140.
[2] M. Bodson & S. C. Douglas, "Adaptive algorithms for the rejection of sinusoidal disturbances with unknown frequency," *Automatica*, vol. 33, no. 12, 1997, pp. 2213-2221.
[3] X. Guo & M. Bodson, "Frequency estimation and tracking of multiple sinusoidal components," *Proc. IEEE Conf. Decision Contr.*, Maui, Hawaii, 2003, pp. 5360-5365.
[4] K. Maertens, J. Schoukens, K. Deprez, & J. D. De Baerdemaeker, "Development of a smart mass flow sensor based on adaptive notch filtering and frequency domain identification," *Proc. of the American Control Conference*, Anchorage, AK, 2002, pp. 4359-4363.
[5] Y. Xu, M. de Mathelin, & D. Knittel, "Adaptive rejection of quasi-periodic tension disturbances in the unwinding of a non-circular roll," *Proc. of the American Control Conference*, Anchorage, AK, 2002, pp. 4009-4014.
[6] Z. Zhao & L. L. Brown, "Musical pitch tracking using internal model control based frequency cancellation," *Proc. IEEE Conf. Decision Contr.*, Maui, Hawaii, 2003, pp. 5544-5548.